INTERPOLATIONS WITH ELASTICAE
IN EUCLIDEAN SPACES

By

W. MIO (*Department of Mathematics, Florida State University, Tallahassee, FL 32306-4510*),

A. SRIVASTAVA (*Department of Statistics, Florida State University, Tallahassee, FL 32306-4330*),

AND

E. KLASSEN (*Department of Mathematics, Florida State University, Tallahassee, FL 32306-4510*)

Abstract. Motivated by interpolation problems arising in image analysis, computer vision, shape reconstruction, and signal processing, we develop an algorithm to simulate curve straightening flows under which curves in $\mathbb{R}^n$ of fixed length and prescribed boundary conditions to first order evolve to *elasticae*, i.e., to (stable) critical points of the elastic energy E given by the integral of the square of the curvature function. We also consider variations in which the length L is allowed to vary and the flows seek to minimize the scale-invariant elastic energy E_{inv}, or the free elastic energy E_λ. E_{inv} is given by the product of L and the elastic energy E, and E_λ is the energy functional obtained by adding a term λ-proportional to the length of the curve to E. Details of the implementations, experimental results, and applications to edge completion problems are also discussed.

1. Introduction. Many applications in signal processing, image analysis, shape reconstruction, and computer vision require interpolation tools in a Riemannian manifold X. One often encounters a collection of points in X, or curves in X with some "missing" pieces, and would like to interpolate curves between them using a set criterion such as the minimization of a cost function that could be given, say, by an energy functional. In this paper, we investigate interpolations based on various elastic energy functionals, to be discussed below. The elastic energy was considered as early as 1738 by D. Bernoulli and investigated by Euler [5].

As an example, in the problem of recognizing objects in a given image, the extraction and use of edges or contours present in the image play an important role. If an object of interest is partially obscured by some others, an important task is to interpolate between the visible edges of the object to complete the hidden contours. In [12], Mumford showed that in the planar case – under a certain Brownian prior for edges – the most likely curves to arise are the ones that are critical points of the (free) elastic energy.

As another example, there is a growing literature on representing images of particular types – such as facial images – as elements of a high-dimensional "image manifold" and using the underlying topology and geometry for image analysis. One idea is to represent images as points in an Euclidean space and locally fit low-dimensional subspaces to images that are clustered together [15]. Each cluster of images is then represented by an element of a real Grassmann manifold G. Interpolation techniques in this manifold can be used to predict properties of unobserved images. For instance, given images of an object taken from azimuthal angles in the $[0, 3\pi/2]$ range, interpolation in G will allow us to predict properties of its image from the angle $7\pi/4$.

The reconstruction of 3D shapes from a series of 2D cross-sections can be viewed as an interpolation problem between points in an infinite-dimensional function space. Jones and Chen [6] represent the contours of the 2D cross-sections as functions using the associated distance fields and use linear interpolations to obtain a function with a 3D domain. The contour of the original 3D shape is reconstructed as an isosurface of this function. Alternative interpolation techniques yield variants of this construction that may produce smoother shapes and incorporate important additional features such as the dependence of the interpolating surfaces on more than two adjacent slices, thus yielding reconstructions that take into account more information about the overall shape of the objects.

In this paper, we study interpolations in Euclidean spaces. We take a geometric approach that, in principle, will apply to general Riemannian manifolds, as the qualitative results of [11] indicate. In this preliminary discussion, we assume that all curves are smooth. The actual class to be considered will be made precise later. Let $\alpha \colon [a, b] \to \mathbb{R}^n$ be a curve parameterized by arc length, i.e., satisfying $\|\alpha'(s)\| = 1$, for every $s \in [a, b]$. The *curvature* of α at s is given by $\kappa(s) = \|\alpha''(s)\|$ and the *elastic energy* E of α is defined by

$$E(\alpha) = \frac{1}{2} \int_a^b \kappa^2(s) \, ds.$$

Among all smooth curves α of a given fixed length L satisfying prescribed boundary conditions to first order, we are interested in those that are critical points of the energy functional E. These curves are known as *elasticae*. After scaling, we may assume that $L = 1$. Hence, we consider curves $\alpha \colon I \to \mathbb{R}^n$ parameterized by arc length, where $I = [0, 1]$. More precisely, given two points $p_0, p_1 \in \mathbb{R}^n$ with $\|p_1 - p_0\| < 1$ and unit vectors $v_0, v_1 \in \mathbb{R}^n$, we are interested in the (stable) critical points of the functional E restricted to curves $\alpha \colon I \to \mathbb{R}^n$ satisfying $\alpha(i) = p_i$ and $\alpha'(i) = v_i$, for $i = 0, 1$. If $\|p_1 - p_0\| = 1$, then a solution exists if and only if $v_0 = v_1 = (p_1 - p_0)/\|p_1 - p_0\|$, and is given by a straight line segment.

Associated with α, there is a *tangent indicatrix* or *direction function* $v\colon I \to \mathbb{S}^{n-1} \subset \mathbb{R}^n$ given by $v(s) = \alpha'(s)$, as illustrated in Fig. 1. The elastic energy of α can be expressed as $E = \frac{1}{2}\int_0^1 v_s \cdot v_s \, ds$.

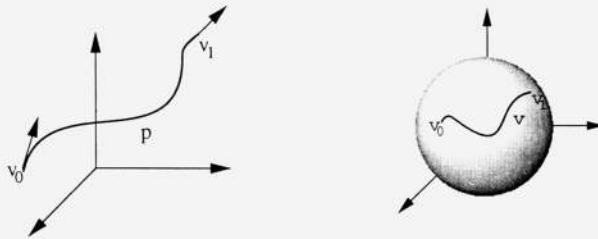

FIG. 1. The direction function associated with a curve in $\mathbb{R}^3$.

Curves with $\alpha(0) = p_0$ are determined by their direction functions via the expression $\alpha(s) = p_0 + \int_0^s v(u)\,du$. The boundary conditions on α can be rephrased as $v(0) = v_0$, $v(1) = v_1$, and $\int_0^1 v(s)\,ds = d$, where $d = p_1 - p_0$ is the total displacement of α. This last condition ensures that the end point of the curve α is p_1.

We treat E as an energy functional defined on mappings $v\colon I \to \mathbb{S}^{n-1}$ and consider its restriction to the infinite-dimensional manifold $\mathcal{M}$ formed by direction functions satisfying the three constraints above. We are interested in the flow on $\mathcal{M}$ associated with the negative gradient field $-\nabla_{\mathcal{M}}E$. Flows that seek to minimize the elastic energy efficiently are known as *curve straightening flows*. We take a computational approach and our main goal is to develop an algorithm to simulate the flow on $\mathcal{M}$ associated with $-\nabla_{\mathcal{M}}E$, whose flow lines approach elasticae asymptotically.

We also consider variations of this problem in which curves satisfy identical boundary conditions, but the length is allowed to vary. In this context, we consider two types of energy functionals:

   (i) the *scale-invariant* elastic energy $E_{inv} = L \cdot E$, where L denotes the length of the curve;

   (ii) the *free* elastic energy $E_\lambda = E + \lambda L$, where $\lambda > 0$.

Critical points of these functionals are known as *scale-invariant elasticae* and *free elasticae*, respectively. Notice that as the value of the parameter λ increases, the contribution of the length L to the free elastic energy becomes more pronounced, so that it is natural to expect that elasticae minimizing E_λ will start to resemble straight lines. This is illustrated by experiments described in Sec. 6. The scale-invariant energy was introduced in [18, 1].

Energy minimizing elasticae are determined by first order boundary conditions. Therefore, when used as interpolating curves, they disregard many geometric properties of the curves to be completed which may be relevant to a specific set of problems. One potential advantage of the present geometric approach to curve straightening flows is that it is, in principle, possible to incorporate further geometric restrictions on the curves under consideration to reflect the known history of the curve we are trying to complete. This problem will be investigated in a future paper.

For closed curves, the qualitative properties of the flow in $\mathbb{R}^n$ associated with $-\nabla_{\mathcal{M}} E$ have been investigated by Langer and Singer [10]. In particular, they study the stability of closed elasticae in $\mathbb{R}^n$ and establish the long-term existence of flow lines. The arguments can be easily adapted to show long-time existence of flow lines in the more general case. Variants of this flow use different spaces of curves and metrics. For closed curves, they have been studied in the planar case by Wen [20] and Koiso [8], and by Dziuk, Kuwert, and Schätzle in $\mathbb{R}^n$ [3], using different techniques. The investigation of elasticae was pioneered by Euler [5] in his work on elastic properties of rods. The reader may consult [17] for a survey of early developments. More recent studies also include work by Bryant and Griffiths [2], Langer and Singer [9, 11], Jurdjevic [7], and Mumford [12]. Other references can be found in the aforementioned articles.

This paper is organized as follows. In Sec. 2, we study the geometric properties of the manifold $\mathcal{M}$, which will be needed in the development of our algorithms. Sec. 3 is devoted to the calculation of the gradient field on $\mathcal{M}$ associated with E. In Sec. 4, we present the implementation details in the length constrained case and some experimental results. The reader will notice that many standard numerical calculations employed in Sec. 4 can be easily modified for more efficiency or accuracy. Our intention was to keep the details as simple as possible to not obscure the main argument. In Secs. 5 and 6, we extend the results to elastic curves of variable length. In the last section, we discuss applications to edge completion problems.

2. A moduli space of curves.

For technical reasons, instead of working only with smooth functions, we consider the vector space $\mathcal{H}$ of all absolutely continuous functions with square integrable derivatives, i.e., the collection of all functions $f : I \to \mathbb{R}^n$ whose derivatives exist almost everywhere and $\int_0^1 \|f'(s)\|^2 \, ds$ is well defined. Define an inner product on $\mathcal{H}$ by

$$\langle f, g \rangle_1 = f(0) \cdot g(0) + \int_0^1 f'(s) \cdot g'(s) \, ds.$$

We use the symbol $\cdot$ to denote the standard inner product on $\mathbb{R}^n$ and $\langle \, , \, \rangle_1$ for the inner product on $\mathcal{H}$. The inner product $\langle , \rangle_1$ has properties analogous to the perhaps more familiar Sobolev inner product $\int_0^1 f(s) \cdot g(s) \, ds + \int_0^1 f'(s) \cdot g'(s) \, ds$, but it better suits our calculations. $\mathcal{H}$ equipped with this inner product is an infinite dimensional Hilbert space.

2.1. *The manifold $\mathcal{C}$.* Let $\mathcal{C}$ be the collection of all absolutely continuous functions $v : I \to \mathbb{S}^{n-1} \subset \mathbb{R}^n$ with square integrable derivative as a function into $\mathbb{R}^n$. $\mathcal{C}$ can be naturally viewed as a metric subspace of $\mathcal{H}$ and is known to be a smooth infinite dimensional manifold. For most purposes, the reader may think of elements of $\mathcal{C}$ as smooth maps.

In order to describe the tangent vectors to the manifold $\mathcal{C}$ at $v_0 : I \to \mathbb{S}^{n-1}$, we first recall how this can be done for a finite dimensional manifold $M \subseteq \mathbb{R}^N$ such as a smooth surface in $\mathbb{R}^3$. If $p \in M$, then any element w of the tangent space $T_p M$ can be written as a velocity vector $w = \alpha'(0)$, where $\alpha : (-\epsilon, \epsilon) \to M$ is a smooth path in M with $\alpha(0) = p$. We do the same in $\mathcal{C}$. If $v_0 \in \mathcal{C}$, a small path in $\mathcal{C}$ through v_0 is known as a *variation* of v_0. More precisely, a variation of v_0 is a map $v : I \times (-\epsilon, \epsilon) \to \mathbb{S}^{n-1}$ such that:

(a) $v(s,0) = v_0(s)$, for every $s \in I$;

(b) the time t map $v^t \colon I \to \mathbb{S}^{n-1}$ given by $v^t(s) = v(s,t)$ is in $\mathcal{C}$, $\forall t \in (-\epsilon, \epsilon)$;

(c) the map $(-\epsilon, \epsilon) \to \mathcal{C}$ given by $t \mapsto v^t$ is smooth.

Any tangent vector f to the manifold $\mathcal{C}$ at v_0 can be described as the time derivative of a variation of v_0 at $t = 0$. Therefore, $f(s) = v_t(s,0) \in T_{v(s)}\mathbb{S}^{n-1}$, for every $s \in I$. As we let s vary, we obtain an absolutely continuous (tangent) vector field with square integrable derivative on $\mathbb{S}^{n-1}$ along the curve v_0. Hence, we will use the expressions tangent vector to $\mathcal{C}$ at v_0 and vector field on $\mathbb{S}^{n-1}$ along v_0 interchangeably.

A vector field f along $v \in \mathcal{C}$ may be viewed as a map $f \colon I \to \mathbb{R}^n$ with the property that $f(s) \perp v(s)$, for every s.

DEFINITION 2.1. The covariant derivative Df of f along v is the vector field along v obtained by projecting the usual derivative of f at s orthogonally onto the tangent space of $\mathbb{S}^{n-1}$ at $v(s)$, for every s. One may interpret Df as the derivative of f from a viewpoint intrinsic to the sphere. A vector field f along v is said to be parallel if $Df \equiv 0$. Parallel fields along curves in $\mathbb{S}^{n-1}$ are the spherical analogues of constant vector fields along curves in $\mathbb{R}^n$.

Now, we introduce a Riemannian structure on $\mathcal{C}$; i.e., we define an inner product on each tangent space $T_v\mathcal{C}$ that varies smoothly on $\mathcal{C}$. Instead of using the inner product that $T_v\mathcal{C}$ inherits from $\mathcal{H}$, we use a variant of $\langle\,,\rangle_1$ that is intrinsic to $\mathcal{C}$. Let f, g be vector fields on $\mathbb{S}^{n-1}$ along v. The inner product of f and g is defined by

$$\langle f, g \rangle = f(0) \cdot g(0) + \int_0^1 Df(s) \cdot Dg(s)\, ds.$$

The manifold $\mathcal{C}$ is *complete* with respect to the metric $\langle\,,\rangle$ since $\mathcal{C}$ includes all absolutely continuous curves $v \colon I \to \mathbb{S}^{n-1}$ with square integrable derivative.

2.2. *The moduli space $\mathcal{M}$.* As discussed in Sec. 1, we are interested in direction functions satisfying the constraints $v(0) = v_0$, $v(1) = v_1$, and $\int_0^1 v(s)\, ds = d$. Therefore, we define a map $\phi \colon \mathcal{C} \to \mathbb{S}^{n-1} \times \mathbb{S}^{n-1} \times \mathbb{R}^n$ by

$$\phi(v) = \big(\phi^1(v), \phi^2(v), \phi^3(v)\big) = \Big(v(0), v(1), \int_0^1 v(s)\, ds\Big),$$

and let $\mathcal{M} = \phi^{-1}(a)$, where $a = (v_0, v_1, d)$. If $\|d\| < 1$, $\mathcal{M}$ is non-empty and consists of the absolutely continuous maps $v \colon I \to \mathbb{S}^{n-1}$ with square integrable derivative satisfying the desired constraints.

REMARK 2.2. The functions $f \mapsto f(0)$ and $f \mapsto f(1)$ that evaluate f at the end points are not continuous on the space of all square integrable functions with the usual $\mathbb{L}^2$-norm. This is one of the reasons why we consider absolute continuous functions and use the inner products $\langle\,,\rangle_1$ and $\langle\,,\rangle$ on $\mathcal{H}$ and $T_v\mathcal{C}$, respectively. •

A geometric argument outlined below shows that $d\phi_v \colon T_v\mathcal{C} \to T_{\phi^1(v)}\mathbb{S}^{n-1} \times T_{\phi^2(v)}\mathbb{S}^{n-1} \times \mathbb{R}^n$ is surjective, for any $v \in \mathcal{C}$. Therefore, if $\|d\| < 1$, $\mathcal{M}$ is a submanifold of $\mathcal{C}$ of codimension $3n - 2$. Here is a sketch of the argument. Let $\alpha \colon I \to \mathbb{R}^n$ be a curve such that $\alpha'(s) = v(s)$ and $\alpha(0) = p_0$. Given $0 \neq w_1 \in T_{\phi^1(v)}\mathbb{S}^{n-1}$, we construct a variation of v such that $d\phi_v(f) = (w_1, 0, 0)$, where $f = v_t(s,0)$. Let $O^t(v(0), w_1)$ be the orthogonal transformation of $\mathbb{R}^n$ which rotates the plane $v(0) - w_1$ by an angle $t\|w_1\|$ and is the identity on its orthogonal complement. Let $R^t = R^t(p_0, v(0), w_1)$ be the corresponding

rotation of $\mathbb{R}^n$ centered at p_0. Then, a variation of α which coincides with R^t in a small neighborhood of $\alpha(0)$ and is the identity on a neighborhood of $\alpha(1)$ will induce a variation of v with the desired properties. Similarly, we show that any vector of the form $(0, w_2, 0)$ is in the image of $d\phi_v$. To conclude, consider vectors of the form $(0, 0, w_3)$ with $w_3 \in \mathbb{R}^n$. In this case, it suffices to consider a variation of α which coincides with translations of $\mathbb{R}^n$ by tw_3 in a small neighborhood of $\alpha(1)$ and is the identity on a neighborhood of $\alpha(0)$.

Let f be a vector field representing a tangent vector to $\mathcal{M}$ at v. Then, f can be written as $f(s) = v_t(s, 0)$, where $v(s, t)$ is a variation satisfying the constraints $v(0, t) = v_0$, $v(1, t) = v_1$, and $\int_0^1 v(s, t)\, ds = d$, for every t. Differentiating these with respect to t at $t = 0$, we obtain the corresponding constraints on f and conclude that f is tangent to $\mathcal{M}$ at v if and only if $f(0) = 0$, $f(1) = 0$, and $\int_0^1 f(s)\, ds = 0$.

2.3. *The derivative of ϕ.* We now compute the derivative of ϕ explicitly. This will allow us to rewrite the three conditions on f in terms of the inner product $\langle\,,\rangle$. In particular, we will be able to exhibit a basis for the fiber of the normal bundle of $\mathcal{M}$ in $\mathcal{C}$ at v and calculate the gradient of the elastic energy functional E on $\mathcal{M}$. The following well-known lemma on covariant integration will be needed in our argument.

LEMMA 2.3. *Let $f(s)$ be a square integrable vector field on $\mathbb{S}^{n-1}$ along the curve $v: I \to \mathbb{S}^{n-1}$, $v \in \mathcal{C}$. Given a tangent vector F_0 to $\mathbb{S}^{n-1}$ at the point $v(0)$, there is a unique absolutely continuous vector field $F(s)$ on $\mathbb{S}^{n-1}$ along v with square integrable derivative such that $F(0) = F_0$ and $DF(s) = f(s)$, almost everywhere.*

Proof. We only present a proof of the lemma in the smooth case, since the differential equation that yields the solution will be used in our simulations. Viewing F as a map into $\mathbb{R}^n$, we can rewrite the differential equation $DF = f$ as

$$F'(s) = f(s) + a(s)v(s), \qquad (2.1)$$

where $a(s)$ is a scalar function to be determined. For a solution F of Eq. 2.1 to induce a vector field on $\mathbb{S}^{n-1}$, we must have $F(s) \cdot v(s) = 0$, for every s. Differentiating this, we obtain $F'(s) \cdot v(s) + F(s) \cdot v'(s) = 0$, or $F'(s) \cdot v(s) = -F(s) \cdot v'(s)$. Hence, we must have

$$-F(s) \cdot v'(s) = F'(s) \cdot v(s) = (f(s) + a(s)v(s)) \cdot v(s) = a(s).$$

Therefore, Eq. 2.1 can be written as

$$F'(s) = -(v'(s) \cdot F(s))\, v(s) + f(s),$$

which is a non-homogeneous linear equation and therefore admits a unique global solution for any given initial condition. $\qquad \square$

2.3.1. *The derivative of ϕ^1.* Let f be a tangent vector to $\mathcal{C}$ at v. Write $f(s) = v_t(s, 0)$, where $v(s, t)$ is a variation of v. Here, we are abusing notation and calling the variation v as well. Differentiating $\phi^1(v(s, t)) = v(0, t)$ with respect to t at $t = 0$, we obtain

$$d\phi_v^1(f) = v_t(0, 0) = f(0).$$

We wish to write $f(0)$ in terms of the inner product $\langle\,,\rangle$. Let $\{e_0^1, e_0^2, \ldots, e_0^{n-1}\}$ be an orthonormal basis of $T_{v(0)}\mathbb{S}^{n-1}$. Abusing notation, for $i = 1, \ldots, n-1$, let $e_0^i(s)$ denote the unique parallel field along v with $e_0^i(0) = e_0^i$. (It is well-known that

$\{e_0^1(s), e_0^2(s), \ldots, e_0^{n-1}(s)\}$ is an orthonormal basis of $T_{v(s)}\mathbb{S}^{n-1}$, for every $s \in I$.) Then, we can write

$$d\phi_v^1(f) = f(0) = \sum_{i=1}^{n-1} \left(f(0) \cdot e_0^i(0)\right) e_0^i(0) = \sum_{i=1}^{n-1} \left\langle f, e_0^i \right\rangle e_0^i(0).$$

This is the desired expression for $d\phi_v^1$ in terms of $\langle \, , \rangle$.

2.3.2. *The derivative of ϕ^2.* In order to compute $d\phi_v^2(f) = f(1)$, we express it in the orthonormal basis $\{e_0^1(1), e_0^2(1), \ldots, e_0^{n-1}(1)\}$ of $T_{v(1)}\mathbb{S}^{n-1}$ as

$$f(1) = \sum_{i=1}^{n-1} \left(f(1) \cdot e_0^i(1)\right) e_0^i(1).$$

We write the coefficients $f(1) \cdot e_0^i(1)$ as follows:

$$\begin{aligned} f(1) \cdot e_0^i(1) - f(0) \cdot e_0^i(0) &= \int_0^1 \frac{d}{ds} \left(f(s) \cdot e_0^i(s)\right) ds \\ &= \int_0^1 Df(s) \cdot e_0^i(s) \, ds \\ &= \left\langle f, se_0^i \right\rangle. \end{aligned} \tag{2.2}$$

Here, we used the fact that $e_0^i(s)$ is parallel and $D(se_0^i)(s) = e_0^i(s)$. This implies that

$$f(1) \cdot e_0^i(1) = f(0) \cdot e_0^i(0) + \left\langle f, se_0^i \right\rangle = \left\langle f, e_0^i \right\rangle + \left\langle f, se_0^i \right\rangle = \left\langle f, e_0^i + se_0^i \right\rangle.$$

Hence,

$$d\phi_v^2(f) = f(1) = \sum_{i=1}^{n-1} \left\langle f, e_0^i + se_0^i \right\rangle e_0^i(1). \tag{2.3}$$

2.3.3. *The derivative of ϕ^3.* Since $\phi^3(v) = \int_0^1 v(s) \, ds$, we have that

$$d\phi_v^3(f) = \int_0^1 f(s) \, ds.$$

Let $\{e_1^1, e_1^2, \ldots, e_1^n\}$ be an orthonormal basis of $\mathbb{R}^n$. For each $s \in I$, project e_1^j orthogonally onto the tangent space of $\mathbb{S}^{n-1}$ at $v(s)$ to obtain vector fields $e_j(s)$ on $\mathbb{S}^{n-1}$ along v. Write $f(s)$ as

$$f(s) = \sum_{j=1}^n \left(f(s) \cdot e_1^j\right) e_1^j = \sum_{j=1}^n (f(s) \cdot e_j(s)) e_1^j.$$

Then,

$$d\phi_v^3(f) = \int_0^1 f(s) \, ds = \sum_{j=1}^n \left(\int_0^1 f(s) \cdot e_j(s) \, ds\right) e_1^j. \tag{2.4}$$

Let $E_j(s)$ be the (unique) vector field along v such that $DE_j(s) = e_j(s)$ and $E_j(0) = 0$. The existence of E_j is guaranteed by Lemma 2.3. Integrating by parts, we obtain

$$
\begin{aligned}
\int_0^1 f(s) \cdot e_j(s)\, ds &= (f(s) \cdot E_j(s))\big|_0^1 - \int_0^1 Df(s) \cdot E_j(s)\, ds \\
&= f(1) \cdot E_j(1) - \int_0^1 Df(s) \cdot E_j(s)\, ds \\
&= f(1) \cdot E_j(1) - \langle f, \varepsilon_j \rangle,
\end{aligned}
\tag{2.5}
$$

where $\varepsilon_j(s)$ is the vector field along v satisfying $D\varepsilon_j(s) = E_j(s)$ and $\varepsilon_j(0) = 0$. By Eq. 2.3,

$$
f(1) = \sum_{k=1}^{n-1} \langle f, e_0^k + se_0^k \rangle\, e_0^k(1).
$$

Therefore,

$$
f(1) \cdot E_j(1) = \sum_{k=1}^{n-1} \langle f, e_0^k + se_0^k \rangle \left(e_0^k(1) \cdot E_j(1) \right).
$$

Using this in (2.5), we obtain

$$
\begin{aligned}
\int_0^1 f(s) \cdot e_j(s)\, ds &= \sum_{k=1}^{n-1} \langle f, e_0^k + se_0^k \rangle \left(e_0^k(1) \cdot E_j(1) \right) - \langle f, \varepsilon_j \rangle \\
&= \left\langle f, \sum_{k=1}^{n-1} a_{jk}(e_0^k + se_0^k) \right\rangle - \langle f, \varepsilon_j \rangle \\
&= \left\langle f, \left(\sum_{k=1}^{n-1} a_{jk}(e_0^k + se_0^k) \right) - \varepsilon_j \right\rangle,
\end{aligned}
\tag{2.6}
$$

where $a_{jk} = e_0^k(1) \cdot E_j(1)$. Hence, by Eq. 2.4,

$$
d\phi_v^3(f) = \sum_{j=1}^n \left\langle f, \left(\sum_{k=1}^{n-1} a_{jk}(e_0^k + se_0^k) \right) - \varepsilon_j \right\rangle e_1^j.
$$

We summarize our calculations in the following proposition.

PROPOSITION 2.4. Let $v \in \mathcal{C}$, and let $f(s)$ be a vector field on $\mathbb{S}^{n-1}$ along v. If $h_j = \left(\sum_{k=1}^{n-1} a_{jk}(e_0^k + se_0^k) \right) - \varepsilon_j$, $1 \leq j \leq n$, then

$$
d\phi_v^1(f) = \sum_{i=1}^{n-1} \langle f, e_0^i \rangle\, e_0^i(0); \qquad d\phi_v^2(f) = \sum_{i=1}^{n-1} \langle f, e_0^i + se_0^i \rangle\, e_0^i(1);
$$

$$
d\phi_v^3(f) = \sum_{i=1}^n \langle f, h_j \rangle\, e_1^j.
$$

THEOREM 2.5. The map $\phi \colon \mathcal{C} \to \mathbb{S}^{n-1} \times \mathbb{S}^{n-1} \times \mathbb{R}^n$ has the property that $d\phi_v \colon T_v \mathcal{C} \to T_{\phi^1(v)}\mathbb{S}^{n-1} \times T_{\phi^2(v)}\mathbb{S}^{n-1} \times \mathbb{R}^n$ is surjective, for any $v \in \mathcal{C}$. If $v_0, v_1 \in \mathbb{S}^{n-1}$, $d \in \mathbb{R}^n$ and $\|d\| < 1$, then the moduli space $\mathcal{M} = \mathcal{M}(v_0, v_1, d) = \phi^{-1}(v_0, v_1, d)$ is a (framed)

submanifold of $\mathcal{C}$ of codimension $3n - 2$. Moreover, the vector fields e_0^i, se_0^i, $1 \leq i \leq n - 1$, and ε_j, $1 \leq j \leq n$, form a basis of the orthogonal complement N_v of the kernel of $d\phi_v$ in $T_v\mathcal{C}$. In particular, for any $v \in \mathcal{M}$, these vectors form a basis of the fiber of the normal bundle of $\mathcal{M}$ in $\mathcal{C}$.

Proof. It only remains to show that the vector fields $e_0^i(s)$, $se_0^i(s)$, and $\varepsilon_j(s)$ span N_v. By Proposition 2.4, a vector field f on $\mathbb{S}^{n-1}$ along v is in the kernel of $d\phi_v$ if and only if the following conditions are satisfied:

   (i) $\langle f, e_0^i \rangle = 0$, for $i = 1, \ldots, n - 1$;
   (ii) $\langle f, e_0^i + se_0^i \rangle = 0$, for $i = 1, \ldots, n - 1$;
   (iii) $\langle f, h_j \rangle = 0$, for $j = 1, \ldots, n$.

Therefore, the vector fields e_0^i, $e_0^i + se_0^i$, and $h_j = \sum_{k=1}^{n-1} a_{jk}(e_0^k + se_0^k) - \varepsilon_j$ span N_v. Since these span the same linear subspace of $T_v\mathcal{C}$ as e_0^i, se_0^i, and ε_j, the result follows. $\qquad\square$

3. The gradient of the elastic energy.

As a functional on $\mathcal{C}$, the elastic energy E of $v \colon I \to \mathbb{S}^{n-1}$ can be expressed as

$$E(v) = \frac{1}{2} \int_0^1 v_s \cdot v_s \, ds. \tag{3.1}$$

We are interested in the gradient of E restricted to the moduli space $\mathcal{M}$. Given a tangent vector f to $\mathcal{C}$ at v, we write it as $f(s) = v_t(s, 0)$, for some variation v. Differentiating (3.1), we obtain

$$dE(f) = \int_0^1 v_s \cdot v_{st} \, ds = \int_0^1 v_s \cdot f_s \, ds = \int_0^1 v_s \cdot Df \, ds. \tag{3.2}$$

The last equality comes from the fact that v_s is tangent to $\mathbb{S}^{n-1}$ at $v(s)$.

Let $Y(s)$ be a vector field on $\mathbb{S}^{n-1}$ along v such that $DY = v_s$ and $Y(0) = 0$, whose existence is guaranteed by Lemma 2.3. Then, we can write Eq. 3.2 as

$$dE(f) = \int_0^1 DY \cdot Df \, ds = \langle Y, f \rangle. \tag{3.3}$$

We view Y as a tangent vector to $\mathcal{C}$ at v. If $v \in \mathcal{M}$ and $f \in T_v\mathcal{M}$, let X be the orthogonal projection of Y onto $T_v\mathcal{M}$. Then, $dE(f) = \langle Y, f \rangle = \langle X, f \rangle$. Therefore,

$$\nabla_{\mathcal{M}} E(s) = X(s); \tag{3.4}$$

i.e., the vector field X along v is the gradient of $E \colon \mathcal{M} \to \mathbb{R}$ at v.

We are interested in the flow on $\mathcal{M}$ associated with the negative gradient field $-\nabla_{\mathcal{M}} E$. Flows of this type that seek to minimize the elastic energy efficiently are known as *curve straightening flows*. For closed curves (with $p_0 = p_1$ and $v_0 = v_1$), a qualitative analysis was carried out by Langer and Singer in [10]. They show that the energy functional E satisfies a property known as the Palais-Smale condition [13, 14] which, among other things, guarantees the long-term existence of flow lines. The arguments can be easily adapted to show that the same is true in the more general setting.

4. Algorithms and Experimental Results. We take a computational approach to finding the optimal curves given by limiting elasticae. In our simulations, we start with a curve in $\mathcal{C}$, project it onto $\mathcal{M}$ so that the constraints $v(0) = v_0$, $v(1) = v_1$, and $\int_0^1 v(s)\,ds$ are satisfied, and let it evolve under the flow associated with the negative gradient field $-\nabla_{\mathcal{M}}E$. First order local approximations to flow lines are used so that they may move points slightly off the manifold $\mathcal{M}$. To account for this, projections back onto $\mathcal{M}$ are used at each step. There are two main computational tasks involved:

(i) to project paths $v \in \mathcal{C}$ onto the manifold $\mathcal{M}$ to initialize the process and keep the flow lines in $\mathcal{M}$;

(ii) to compute the gradient vectors $\nabla_{\mathcal{M}}E$ for the updates.

We now describe the details of the implementation. To represent a direction function $v\colon I \to \mathbb{S}^{n-1}$ on a digital computer, we divide the interval $[0,1]$ into T equal segments of size $\Delta = 1/T$ and use a discretized version of $v \in \mathcal{C}$ given by $\{\tilde{v}(s),\ s = 0, 1, \ldots, T\}$. We adopt this convention in general: given a function α defined on the interval I, $\tilde{\alpha}$ will denote its discretization.

4.1. *Integrating Vector Fields.* Given a vector field f along v, Lemma 2.3 gives a vector field F along v such that $DF = f$ and $F(0) = F_0$. We use the following discretized computation:

$$\tilde{F}(s+1) = \tilde{F}(s) + \Delta(\tilde{f}(s) - (\tilde{v}_s \cdot \tilde{F}(s))\tilde{v}(s)). \tag{4.1}$$

The vector field $\tilde{v}_s$ is computed using $\tilde{v}_s(s) = (\tilde{v}(s+1) - \tilde{v}(s))/\Delta$. Equation 4.1 is used to compute the discretized vector fields $\tilde{E}_j$, $j = 1, \ldots, n$ and $\tilde{\epsilon}_j$, $j = 1, \ldots, n$.

4.2. *Computation of the Jacobian.* To project a curve $v \in \mathcal{C}$ onto $\mathcal{M}$, we use the derivative $d\phi_v$ restricted to the $(3n-2)$-dimensional subspace N_v orthogonal to the kernel of $d\phi_v$. Proposition 2.4 shows how to compute the Jacobian matrix J using the basis of N_v formed by the vectors $\tilde{e}_0^k$, $s\tilde{e}_0^k$, and $\tilde{\epsilon}_j$, where $1 \le k \le n-1$ and $1 \le j \le n$. For the tangent space $T_{\phi(v)}(\mathbb{S}^{n-1} \times \mathbb{S}^{n-1} \times \mathbb{R}^n) = T_{\phi^1(v)}\mathbb{S}^{n-1} \times T_{\phi^2(v)}\mathbb{S}^{n-1} \times \mathbb{R}^n$, we use the basis formed by $(e_0^k(0), 0, 0)$, $(0, e_0^k(1), 0)$, and the standard basis of $\mathbb{R}^n$.

For $k = 1, \ldots, n-1$ and $i, j = 1, \ldots, n$, define the following scalars:

$$a_{jk} = \tilde{e}_0^k(T) \cdot \tilde{E}_j(T);$$

$$b_{jk} = \int_0^1 e_0^k(s) \cdot E_j(s)\,ds \sim \Delta\left(\sum_{s=0}^{T-1} \tilde{e}_0^k(s) \cdot \tilde{E}_j(s)\right);$$

$$c_{ij} = \int_0^1 E_i(s) \cdot E_j(s)\,ds \sim \Delta\left(\sum_{s=0}^{T-1} \tilde{E}_i(s) \cdot \tilde{E}_j(s)\right).$$

Both $a = (a_{jk})$ and $b = (b_{jk})$ are $n \times (n-1)$ matrices, and $c = (c_{ij})$ is an $n \times n$ matrix. In this notation, the Jacobian J is given by the following $(3n-2) \times (3n-2)$ matrix:

$$J = \begin{bmatrix} I_{n-1} & 0 & 0 \\ I_{n-1} & I_{n-1} & b^T \\ a & a-b & ab^T - c \end{bmatrix}. \tag{4.2}$$

4.3. *Projecting a path v onto $\mathcal{M}$.* One of our tasks is to start with a point $v \in \mathcal{C}$ and iteratively project it onto the manifold $\mathcal{M}$. Recall that φ maps $\mathcal{C}$ to the space $\mathbb{S}^{n-1} \times$

$\mathbb{S}^{n-1} \times \mathbb{R}^n$, while $d\phi_v$ maps the tangent space $T_v(\mathcal{C})$ to the tangent space $T_{\phi(v)}(\mathbb{S}^{n-1} \times \mathbb{S}^{n-1} \times \mathbb{R}^n)$, as illustrated in Fig. 2.
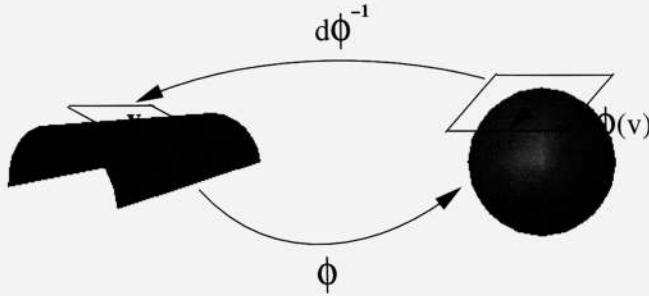

FIG. 2. ϕ maps the manifold $\mathcal{C}$ to $\mathbb{S}^{n-1} \times \mathbb{S}^{n-1} \times \mathbb{R}^n$, while $d\phi_v$ maps the tangent space $T_v(\mathcal{C})$ onto the tangent space $T_{\phi(v)}(\mathbb{S}^{n-1} \times \mathbb{S}^{n-1} \times \mathbb{R}^n)$.

The basic idea is to evaluate $\phi(v)$ and check how far it is from the desired value $a = (v_0, v_1, d)$ by computing the residual vector $w = (w_1, w_2, w_3) \in T_{\phi(v)}(\mathbb{S}^{n-1} \times \mathbb{S}^{n-1} \times \mathbb{R}^n)$, characterized by the following properties:

(a) for $i = 1, 2$, if we travel $\|w_i\|$ units of length along the great circle on $\mathbb{S}^{n-1}$ starting at $\phi^i(v)$ in the direction of w_i, we reach the point v_{i-1};

(b) $w_3 = d - \phi^3(v)$.

Then, we pull back this residual vector w to $N_v \subset T_v\mathcal{C}$ under J to determine how to move v in $\mathcal{C}$, to first order. The vector w is computed as follows:

$$w_1 = \cos^{-1}(v_0 \cdot \tilde{v}(0)) \frac{u_0}{\|u_0\|}, \quad u_0 = (v_0 - \tilde{v}(0)) - ((v_0 - \tilde{v}(0)) \cdot \tilde{v}(0))\tilde{v}(0);$$

$$w_2 = \cos^{-1}(v_1 \cdot \tilde{v}(T)) \frac{u_1}{\|u_1\|}, \quad u_1 = (v_1 - \tilde{v}(T)) - ((v_1 - \tilde{v}(T)) \cdot \tilde{v}(T))\tilde{v}(T);$$

$$w_3 = \left(d - \int_0^1 v(s)ds\right) \sim d - \Delta \left(\sum_{s=0}^{T-1} \tilde{v}(s)\right).$$

Let $\gamma = (\gamma_1, \ldots, \gamma_{3n-2})$ be the $(3n-2)$-tuple consisting of the coordinates of w in the orthonormal basis formed by the vectors $e_0^k(0)$, $e_0^k(1)$, and the standard basis of $\mathbb{R}^n$, where $1 \le k \le n-1$. The scalars γ_i are given by:

$$\begin{aligned} \gamma_i &= w_1 \cdot \tilde{e}_0^i(0), \quad i = 1, \ldots, n-1; \\ \gamma_{n-1+i} &= w_2 \cdot \tilde{e}_0^i(T), \quad i = 1, \ldots, n-1; \\ \gamma_{2n-2+i} &= w_3(i), \quad i = 1, \ldots, n. \end{aligned} \tag{4.3}$$

4.4. *Updating the Curve v.* Let $\beta = J^{-1}(\gamma)$, and define $\tilde{d}v \in T_v\mathcal{C}$ by

$$\tilde{d}v(s) = \sum_{i=1}^{n-1} \beta_i \tilde{e}_0^i(s) + \sum_{i=1}^{n-1} \beta_{n-1+i} s \tilde{e}_0^i(s) + \sum_{i=1}^{n} \beta_{2n-2+i} \tilde{\varepsilon}_i(s).$$

To update v, as a first order approximation to geodesics in $\mathcal{C}$, for each $s \in \{0, \ldots, T\}$, we follow $\|\tilde{d}v(s)\|$ units of length along the great circle on $\mathbb{S}^{n-1}$ starting at $v(s)$ in the direction of the vector $\tilde{d}v(s)$, as illustrated in Fig. 3. If $\tilde{d}v(s) \neq 0$, then the update is computed as follows:

$$\tilde{v}_{\text{new}}(s) = \cos(\|\tilde{d}v(s)\|)\tilde{v}(s) + \frac{\sin(\|\tilde{d}v(s)\|)}{\|\tilde{d}v(s)\|}\tilde{d}v(s). \tag{4.4}$$
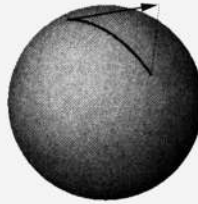

FIG. 3. The arrow represents the tangent vector $dv(s) \in T_{v(s)}\mathbb{S}^{n-1}$. Each $v(s)$ is updated along a great circle.

4.5. *The Gradient of E.* Let $\tilde{Y}$ be the vector field such that $D\tilde{Y} = \tilde{v}_s$ and $\tilde{Y}(0) = 0$, which can be computed using Eq. 4.1. Project $\tilde{Y}$ orthogonally onto $T_v(\mathcal{M})$ to obtain $\tilde{X}$. To implement this, we first apply Gram-Schmidt to $\{\tilde{e}_0^i, s\tilde{e}_0^i, \tilde{\varepsilon}_j\}$ to obtain an orthonormal basis of $T_v\mathcal{C}$. Since $\{\tilde{e}_0^i, s\tilde{e}_0^i\}$ already is an orthonormal set, it suffices to correct the collection $\{\tilde{\varepsilon}_j\}$ to obtain, say, $\{\tilde{\theta}_j\}$. Then, the vector field $\tilde{X}$ is given by:

$$\tilde{X} = \tilde{Y} - \sum_{i=1}^{n-1}\langle\tilde{Y}, \tilde{e}_0^i\rangle\tilde{e}_0^i - \sum_{i=1}^{n-1}\langle Y, \tilde{s}e_0^i\rangle\tilde{s}e_0^i - \sum_{j=1}^{n}\langle\tilde{Y}, \tilde{\theta}_j\rangle\tilde{\theta}_j. \tag{4.5}$$

The algorithmic steps are summarized next.

ALGORITHM 4.1 (Projection onto $\mathcal{M}$). Start with a curve $\tilde{v}$ that is not in $\mathcal{M}$.
    (1) Compute the vector γ according to Eq. 4.3.
    (2) Compute the Jacobian matrix using Eq. 4.2.
    (3) Compute β and update $\tilde{v}$ according to Eq. 4.4. Go to step 1.

ALGORITHM 4.2 (Finding Elasticae). Start with a curve $\tilde{v}$ in $\mathcal{C}$.
    (1) Project it onto the manifold $\mathcal{M}$ using Algorithm 4.1.
    (2) Compute the gradient vector field $\tilde{X}$ according to Eq. 4.5.
    (3) Update the curve $\tilde{v}$ using Eq. 4.4 with $\tilde{X}$ replacing $\tilde{d}v$.
    (4) Go to step 1.

Shown in Fig. 4 are some examples of elasticae satisfying boundary conditions p_0, p_1, v_0, and v_1. To initialize the gradient search, we first randomly generate many curves in $\mathcal{C}$ and select the one for which $\|\phi(v) - a\|$ is minimal. This curve is shown as a broken line in each plot. Next, we project it onto $\mathcal{M}$ using the steps described earlier; this projected curve is our initial condition and is plotted in thin lines. Finally, we perform ten iterations of the gradient flow to reach the elastica drawn as a solid line. Fig. 5 shows some examples of elasticae in $\mathbb{R}^3$.
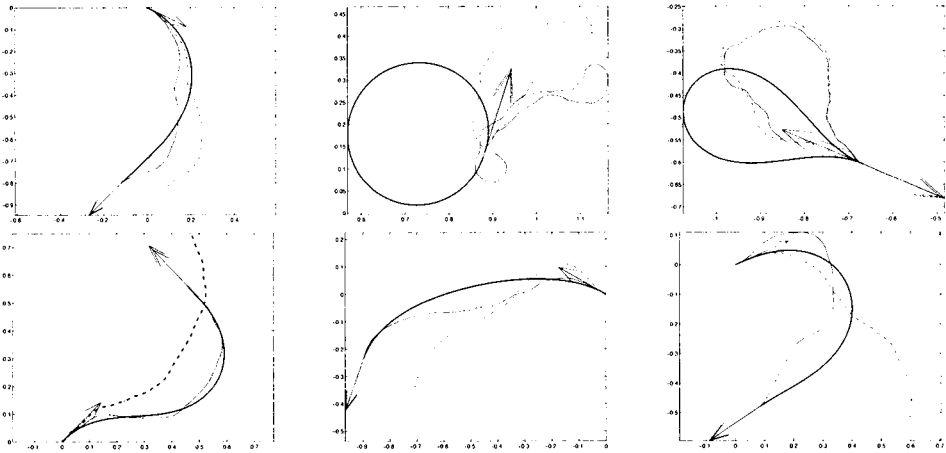
FIG. 4. Elastic curves in $\mathbb{R}^2$: in each panel, the broken line shows an
initial curve in $\mathcal{C}$, the thin line shows its projection onto $\mathcal{M}$, and the
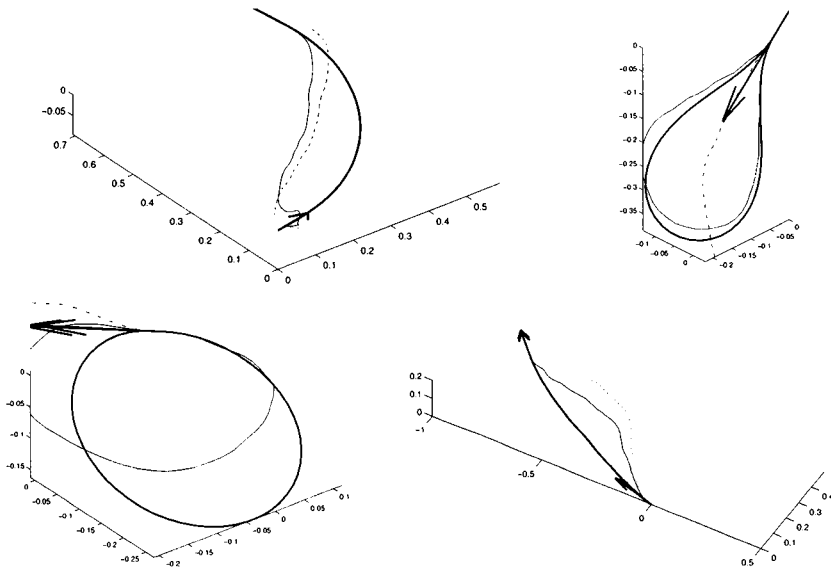solid line shows the elasticae obtained after ten gradient iterations.

FIG. 5. Elastic curves in $\mathbb{R}^3$: broken lines show initial curves in $\mathcal{C}$,
thin lines show their projections onto $\mathcal{M}$, and solid lines show the
elasticae obtained after ten gradient iterations.

REMARK 4.3. To randomly initialize the gradient search as proposed, we need the full
description of residual vectors given above. However, once the curve v is in the manifold
$\mathcal{M}$, the conditions $v(0) = v_0$ and $v(1) = v_1$ are automatically satisfied in subsequent
steps since the gradient vector X has the property that $X(0) = 0$ and $X(1) = 0$. This
means that we may assume that the residual vectors needed during the gradient search
have the simpler form $(0, 0, w_3)$.

5. Scale-invariant and free elasticae. We now consider the analogous problem for curves with prescribed boundary conditions to first order whose lengths are allowed to vary. We only consider curves $\beta\colon I \to \mathbb{R}^n$ parameterized with constant speed. Thus, if the length of β is L, $\|\beta'(s)\| = L$, for every $s \in I$. Let $\alpha\colon I \to \mathbb{R}^n$ be the length-one curve obtained by scaling β by a factor $1/L$ so that $\alpha(s) = \beta(s)/L$, and let $v\colon I \to \mathbb{S}^{n-1}$ be the direction function of α. Given $p_0 \in \mathbb{R}^n$, if we impose the extra condition $\beta(0) = p_0$, then $\beta(s) = p_0 + L \int_0^s v(u)\,du$. This establishes a one-to-one correspondence between the curves β under consideration and pairs $(L, v) \in (0, \infty) \times \mathcal{C}$. If we use a logarithmic scale for the length by writing $L = e^x$, then β is represented by a pair $(x, \alpha) \in \mathbb{R} \times \mathcal{C}$ via the expression $\beta(s) = p_0 + e^x \int_0^s v(u)\,du$.

Given $p_0, p_1 \in \mathbb{R}^n$ and $v_0, v_1 \in \mathbb{S}^{n-1}$, we are interested in curves β satisfying the boundary conditions $\beta(0) = p_0$, $\beta(1) = p_1$, $\beta'(0)/L = v_0$, and $\beta'(1)/L = v_1$. These conditions can be rephrased in terms of the pair (x, v) as $v(0) = v_0$, $v(1) = v_1$, and $\int_0^1 v(s)\,ds = d/e^x$, where $d = p_1 - p_0$. Therefore, we consider the function $\psi\colon \mathbb{R} \times \mathcal{C} \to \mathbb{S}^{n-1} \times \mathbb{S}^{n-1} \times \mathbb{R}^n$ given by

$$\psi(x, v) = \left(v(0), v(1), e^x \int_0^1 v(s)\,ds \right),$$

and define $\mathcal{N} = \psi^{-1}(v_0, v_1, d)$. We are considering $\mathbb{R} \times \mathcal{C}$ with the product metric denoted $(\,,\,)$. The $\mathbb{R}$ factor is endowed with the usual Euclidean metric and $\mathcal{C}$ is equipped with the metric $\langle\,,\,\rangle$ defined in Sec. 2. Hence, if $w_i \in \mathbb{R}$ and f_i is tangent to $\mathcal{C}$ at v, for $i = 0, 1$, then

$$((w_0, f_0), (w_1, f_1)) = w_0 \cdot w_1 + \langle f_0, f_1 \rangle.$$

The adoption of a logarithmic scale for length measurements has the virtue of turning the domain of ψ into a complete Riemannian manifold.

We consider two types of elastic energy functionals for curves of variable length: the *scale-invariant* elastic energy $E_{inv}\colon \mathbb{R} \times \mathcal{C} \to \mathbb{R}$, given by

$$E_{inv}(x, v) = \frac{1}{2} \int_0^1 v_s \cdot v_s\,ds,$$

and, for each $\lambda > 0$, the *free* elastic energy $E_\lambda\colon \mathbb{R} \times \mathcal{C} \to \mathbb{R}$, defined by

$$E_\lambda(x, v) = \frac{1}{2L} \int_0^1 v_s \cdot v_s\,ds + \lambda L$$

$$= \frac{1}{2e^x} \int_0^1 v_s \cdot v_s\,ds + \lambda e^x.$$

The scale-invariant energy of a curve β is simply the elastic energy of the associated normalized length-one curve $\alpha = (1/L)\beta$.

The critical points of the restriction of E_{inv} and E_λ to $\mathcal{N}$ – which we also denote by E_{inv} and E_λ – are called *scale-invariant elasticae* and *free elasticae*, respectively.

As before, a simple geometric argument shows that $d\psi_{(x,v)}$ is surjective. We now compute the derivative of $\psi = (\psi^1, \psi^2, \psi^3)$ explicitly. Any tangent vector to $\mathcal{N}$ at (x, v) is of the form (w, f), where $w \in \mathbb{R}$ and f is a vector field on $\mathbb{S}^{n-1}$ along v. For any point

$(x, v) \in \mathbb{R} \times \mathcal{C}$, the calculations of Sec. 2 imply that

$$d\psi^1(w, f) = f(0) = \sum_{i=1}^{n-1} \langle f, e_0^i \rangle e_0^i(0) = \sum_{i=1}^{n-1} \left((w, f), (0, e_0^i) \right) e_0^i(0)$$

and

$$d\psi^2(w, f) = f(1) = \sum_{i=1}^{n-1} \langle f, e_0^i + s e_0^i \rangle e_0^i(1)$$

$$= \sum_{i=1}^{n-1} \left((w, f), (0, e_0^i + s e_0^i) \right) e_0^i(1).$$

As in Sec. 2, let e_1^j, $1 \le j \le n$, be an orthonormal basis of $\mathbb{R}^n$. Differentiating $\psi^3(x, v) = e^x \int_0^1 v(s)\, ds$ and using Proposition 2.4, we obtain

$$d\psi^3(w, f) = e^x w \int_0^1 v(s)\, ds + e^x \int_0^1 f(s)\, ds$$

$$= e^x w \sum_{j=1}^{n} \left(\int_0^1 v(s) \cdot e_1^j\, ds \right) e_1^j + e^x \sum_{j=1}^{n} \langle f, h_j \rangle e_1^j$$

$$= e^x w \sum_{j=1}^{n} \left(\int_0^1 v_j(s)\, ds \right) e_1^j + e^x \sum_{j=1}^{n} \langle f, h_j \rangle e_1^j$$

$$= e^x \sum_{j=1}^{n} \left((w, f), \left(\int_0^1 v_j(s)\, ds, h_j \right) \right) e_1^j,$$

where $v_j(s) = v(s) \cdot e_1^j$, $h_j = \left(\sum_{k=1}^{n-1} a_{jk} (e_0^k + s e_0^k) \right) - \varepsilon_j$, and $a_{jk} = E_j(1) \cdot e_0^k(1)$, for $1 \le j \le n$. This completes the calculation of $d\psi$ and yields the following analogues of Proposition 2.4 and Theorem 2.5.

PROPOSITION 5.1. Let $(x, v) \in \mathbb{R} \times \mathcal{C}$ and $(w, f) \in \mathbb{R} \times T_v \mathcal{C}$. Then,

$$d\psi^1(w, f) = \sum_{i=1}^{n-1} \left((w, f), (0, e_0^i) \right) e_0^i(0);$$

$$d\psi^2(w, f) = \sum_{i=1}^{n-1} \left((w, f), (0, e_0^i + s e_0^i) \right) e_0^i(1);$$

$$d\psi^3(w, f) = \sum_{j=1}^{n} \left((w, f), e^x \left(\int_0^1 v_j(s)\, ds, h_j \right) \right) e_1^j.$$

THEOREM 5.2. The map $\psi \colon \mathbb{R} \times \mathcal{C} \to \mathbb{S}^{n-1} \times \mathbb{S}^{n-1} \times \mathbb{R}^n$ given by

$$\psi(x, v) = \left(v(0), v(1), e^x \int_0^1 v(s)\, ds \right)$$

has the property that $d\psi_{(x,v)} \colon \mathbb{R} \times T_v \mathcal{C} \to T_{\psi^1(x,v)} \mathbb{S}^{n-1} \times T_{\psi^2(x,v)} \mathbb{S}^{n-1} \times \mathbb{R}^n$ is surjective, for any $(x, v) \in \mathbb{R} \times \mathcal{C}$. If $v_0, v_1 \in \mathbb{S}^{n-1}$ and $d \in \mathbb{R}^n$, then the moduli space $\mathcal{N} = \mathcal{N}(v_0, v_1, d) = \psi^{-1}(v_0, v_1, d)$ is a (framed) submanifold of $\mathbb{R} \times \mathcal{C}$ of codimension $3n - 2$.

Moreover, the vectors $(0, e_0^i)$, $(0, s e_0^i)$, $1 \leq i \leq n - 1$, and $(- \int_0^1 v_j(s) \, ds, \varepsilon_j)$, $1 \leq j \leq n$, form a basis of the orthogonal complement of the kernel of $d\psi_{(x,v)}$, at any $(x, v) \in \mathbb{R} \times \mathcal{C}$. In particular, if $(x, v) \in \mathcal{N}$, these vectors form a basis of the fiber of the normal bundle of $\mathcal{N}$ in $\mathbb{R} \times \mathcal{C}$ at (x, v).

We conclude this section with a calculation of the gradient of $E_{inv} \colon \mathcal{N} \to \mathbb{R}$ and $E_\lambda \colon \mathcal{N} \to \mathbb{R}$. Let (w, f) be a tangent vector to $\mathbb{R} \times \mathcal{C}$ at (x, v). As usual, we write $(w, f) = (x_t, v_t)$ at $t = 0$. Differentiating

$$E_{inv}(x, v) = \frac{1}{2} \int_0^1 v_s \cdot v_s \, ds$$

with respect to t at $t = 0$, and letting Y be the field along v whose covariant derivative is v_s and $Y(0) = 0$, we obtain

$$\begin{aligned}
dE_{inv}(w, f) &= \int_0^1 \langle f_s, v_s \rangle \, ds = \int_0^1 \langle Df, v_s \rangle \, ds = \langle Y, f \rangle \\
&= ((0, Y), (w, f)).
\end{aligned} \tag{5.1}$$

Projecting the vector $(0, Y)$ orthogonally onto the tangent space of $\mathcal{N}$ at (x, v), we obtain the gradient of E_{inv} at (x, v). Similarly, differentiating

$$E_\lambda(x, v) = \frac{1}{2e^x} \int_0^1 v_s \cdot v_s \, ds + \lambda e^x,$$

we obtain

$$\begin{aligned}
dE_\lambda(w, f) &= -\frac{1}{2e^x} \left(\int_0^1 v_s \cdot v_s \, ds \right) w + \frac{1}{e^x} \int_0^1 v_s \cdot f_s \, ds + \lambda e^x w \\
&= \left(-\frac{E(v)}{e^x} + \lambda e^x \right) w + \frac{1}{e^x} \int_0^1 DY \cdot Df \, ds \\
&= \left(-\frac{E(v)}{e^x} + \lambda e^x \right) w + \frac{1}{e^x} \langle Y, f \rangle \\
&= \left(\left(-\frac{E(v)}{e^x} + \lambda e^x, \frac{Y}{e^x} \right), (w, f) \right).
\end{aligned} \tag{5.2}$$

The orthogonal projection of the vector

$$\left(-\frac{E(v)}{e^x} + \lambda e^x, \frac{Y}{e^x} \right)$$

onto $T_{(x,v)}\mathcal{N}$ gives the gradient of E_λ at (x, v).

6. Algorithms and Experimental Results. The computational tasks for variable length elastic curves are similar to the ones discussed in Sec. 4 with a few exceptions that are listed here.

6.1. *Computation of the Jacobian.* In the basis of the orthogonal complement $N_{(x,v)}$ of the kernel of $d\psi_{(x,v)}$ formed by the vectors $(0, e_0^k)$, $(0, se_0^k)$, and $(-\int v_j(s)\,ds, \varepsilon_j)$, the Jacobian matrix of the restriction of $d\psi_{(x,v)}$ to $N_{(x,v)}$ is given by:

$$
J = \begin{bmatrix}
I_{n-1} & 0 & 0 \\
I_{n-1} & I_{n-1} & b^T \\
e^x a & e^x(a-b) & e^x(ab^T - c - gg^T)
\end{bmatrix}, \tag{6.1}
$$

where a, b, and c are as in Sec. 4 and $g = (g_{j1})$ is the $n \times 1$ matrix whose entries are given by $g_{j1} = \int_0^1 v_j(s)\,ds = \int_0^1 v(s) \cdot e_1^j(s)\,ds$. Here, we are using the basis of $T(\mathbb{S}^{n-1} \times \mathbb{S}^{n-1} \times \mathbb{R}^n)$ formed by $e_0^k(0)$, $e_0^k(1)$, and the standard basis of $\mathbb{R}^n$.

6.2. *Projecting (x,v) onto $\mathcal{N}$.* The projection of (x,v) onto $\mathcal{N}$ requires that we compute the residual vector w, which is done as follows:

$$
w_1 = \cos^{-1}(v_0 \cdot \tilde{v}(0))\frac{u_0}{\|u_0\|}, \quad u_0 = (v_0 - \tilde{v}(0)) - ((v_0 - \tilde{v}(0)) \cdot \tilde{v}(0))\tilde{v}(0);
$$

$$
w_2 = \cos^{-1}(v_1 \cdot \tilde{v}(T))\frac{u_1}{\|u_1\|}, \quad u_1 = (v_1 - \tilde{v}(T)) - ((v_1 - \tilde{v}(T)) \cdot \tilde{v}(T))\tilde{v}(T);
$$

$$
w_3 = (d - e^x \int_0^1 v(s)ds) \sim d - e^x \Delta \left(\sum_{s=0}^{T-1} \tilde{v}(s) \right).
$$

The vector γ is the same as in Eq. 4.3.

6.3. *Updating (x,v).* Let $\beta = J^{-1}\gamma$. Then, x is updated as follows:

$$
x_{\text{new}} = x + dx, \quad dx = -\sum_{i=1}^{n} \beta_{2n-2+i} \left(\Delta \left(\sum_{s=0}^{T} \tilde{v}(s) \cdot e_1^i \right) \right). \tag{6.2}
$$

The curve $\tilde{v}$ is updated as before using Eq. 4.4.

6.4. *The Gradient of E_{inv} and E_λ.* Let $\tilde{Y}$ be the vector field such that $D\tilde{Y} = \tilde{v}_s$ and $\tilde{Y}(0) = 0$, computed using Eq. 4.1. By (5.2), to obtain $\nabla_{(x,v)}E_\lambda$, we project the vector $(w_1, \tilde{Y}/e^x)$ orthogonally onto $T_{(x,v)}\mathcal{N}$, where $w_1 = -E(v)/e^x + \lambda e^x$. Let (z_i, Z_i), $i = 1,\ldots,3n-2$, be an orthonormal basis of the subspace spanned by $(0, \tilde{e}_0^i), (0, s\tilde{e}_0^i), (-\int_0^1 v(s)\cdot e_1^j ds, \tilde{\varepsilon}_j)$, which can be obtained using the Gram-Schmidt method. Then, the gradient of E_λ is given by

$$
\nabla_{(x,v)}E_\lambda = (w_1, \frac{\tilde{Y}}{e^x}) - \sum_{i=1}^{3n-2} \left((w_1, \frac{\tilde{Y}}{e^x}), (z_i, Z_i) \right)(z_i, Z_i). \tag{6.3}
$$

A similar calculation yields, using (5.1),

$$
\nabla_{(x,v)}E_{inv} = (0, \tilde{Y}) - \sum_{i=1}^{3n-2} \left((0, \tilde{Y}), (z_i, Z_i) \right)(z_i, Z_i). \tag{6.4}
$$

6.5. *Experimental results.* Shown in Fig. 6 are some examples of free elasticae computed using this approach. The left panel displays the vertices of an equilateral triangle with tangent vectors as shown. The curves represent free elasticae between these points for the values 1, 11, 41, 91, and 161 of the parameter λ. As the value of λ grows, the contribution of the length to the energy becomes more significant and the elasticae become tighter trying to approach the straight line segment connecting the end points, as

expected. A similar result is displayed in the middle panel for two vertically displaced points with horizontal tangents pointing in opposite directions. The last panel shows an example of a free elastica in $\mathbb{R}^3$.
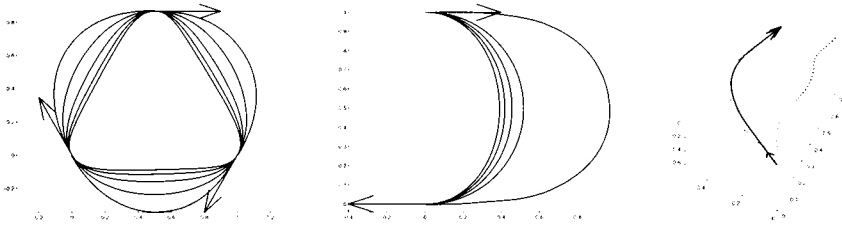

FIG. 6. Free elastic curves: (i) The left panel shows a sequence of free elasticae connecting points in a triangle for several values of the parameter λ. (ii) A similar result for two vertically separated points with opposite horizontal direction vectors. (iii) A free elastica in $\mathbb{R}^3$.

Figure 7 displays several stages of the evolution of a planar curve toward a free elastica and a plot of the corresponding evolution of the free elastic energy.
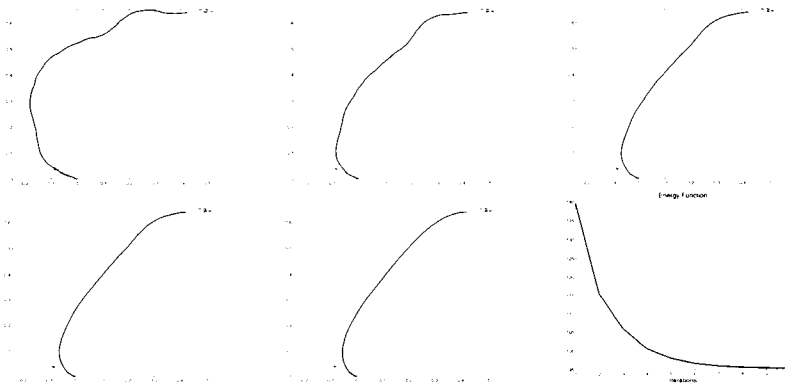

FIG. 7. Several stages of the evolution of a planar curve toward a free elastica and a plot of the corresponding evolution of the free elastic energy.

7. Applications to edge completion. Edge completion is an important application of elasticae to computer vision. If objects of interest in a given image are partially obscured, an important task is to interpolate between the visible edges to complete the hidden contours. Boundaries, or contours, of objects provide important clues in object recognition. The ability of the human visual system to interpolate between the visible edges is well documented and we would like to develop a computational approach to such interpolations.

Shown in Fig. 8 are four examples of edge completion using scale-invariant elasticae. The left panels show images of objects whose contours were extracted using standard edge detection procedures. The middle panels show the same images with some parts

artificially obscured. The right panels show superpositions of the interpolating scale-invariant elasticae and the original contours. The actual boundaries are shown as a broken lines and the completion curves are drawn using solid white lines. The boundary conditions for the interpolating elasticae were estimated using points near the ends of the visible edges.
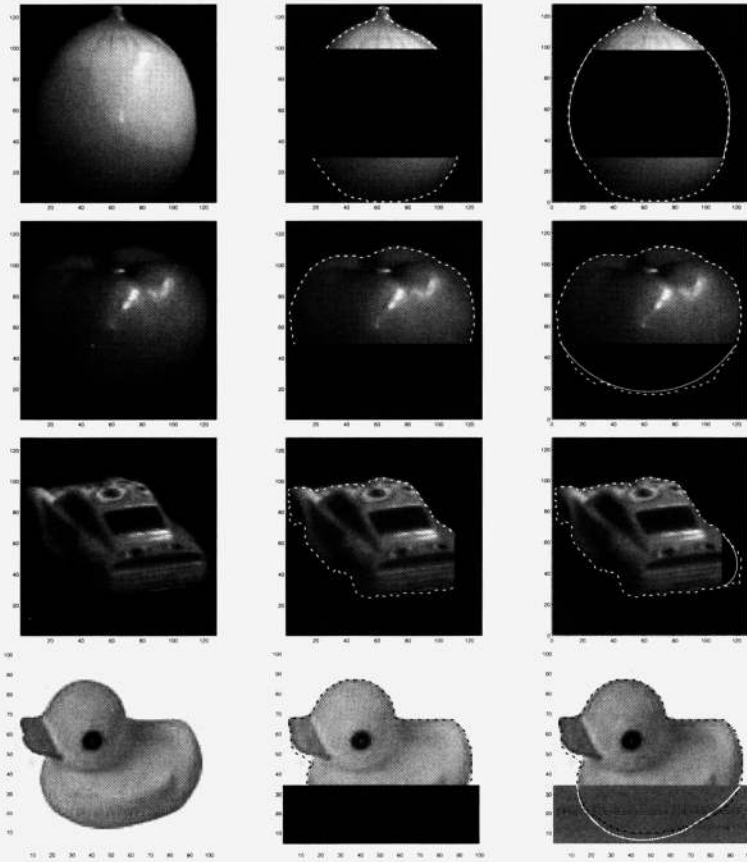

FIG. 8. Edge completion using scale-invariant elasticae.

Several researchers have proposed the use of elasticae for completing partially occluded edges in a statistical framework. In [12], Mumford showed that – under a Brownian prior for edges – the most likely curves to occur are free elasticae. The use of scale-invariant elasticae in this context has been proposed in [4], [19], [16]. Other references can be found in [16]. These statistical formulations are especially useful in situations where several edges are to be completed in the same image and the right pairings of edges are not obvious. In these probabilistic models, one generates *stochastic completion fields* and selects the most likely curves for edge completion. These high probability curves are curves of least elastic energy, which can be produced using the algorithms developed in this paper.

REFERENCES

[1] A. M. Bruckstein and A. N. Netravali, *On minimal energy trajectories*, Computer Vision, Graphics, and Image Processing **49** (1990), 283–396.

[2] R. Bryant and P. Griffiths, *Reduction of order for the constrained variational problem and $\int k^2/2\,ds$*, Amer. J. Math. **108** (1986), 525–570.

[3] G. Dziuk, E. Kuwert, and R. Schätzle, *Evolution of elastic curves in $\mathbb{R}^n$: existence and computation*, SIAM J. Math. Anal. **33** (2002), 1228–1245.

[4] G. Guy and G. Medioni, *Inferring global perceptual contours from local features*, Int'l J. Computer Vision **20** (1996), 113–133.

[5] L. Euler, *Methodus inveniendi lineas curvas maximi minimive proprietate gaudentes, sive solutio problematis isoperimetrici lattisimo sensu accepti*, Bousquet, Lausannae e Genevae **24** (1744) E65A. O. O. Ser. I.

[6] M. W. Jones and M. Chen, *A new approach to the construction of surfaces from contour data*, Computer Graphics Forum **13** (1994), C-85–C-84.

[7] V. Jurdjevic, *Non-Euclidean elastica*, Amer. J. Math. **117** (1995), 93–124.

[8] N. Koiso, *On the motion of a curve towards elastica*, in: Actes de la Table Ronde de Géometrie Différentielle (Luminy 1992) Sémin. Congr. 1 (Soc. Math. France, Paris, 1996), 403–436.

[9] J. Langer and D. A. Singer, *The total squared curvature of closed curves*, J. Differential Geometry **20** (1984), 1–22.

[10] J. Langer and D. A. Singer, *Curve straightening and a minimax argument for closed elastic curves*, Topology **24** (1985), 75–88.

[11] J. Langer and D. A. Singer, *Curve straightening in Riemannian manifolds*, Ann. Global Anal. Geom. **5** (1987), 133–150.

[12] D. Mumford, *Elastica and computer vision*, in: Algebraic Geometry and its Applications (West Lafayette, IN, 1990) (Springer, New York, 1994), 491–506.

[13] R. Palais, *Morse theory on Hilbert manifolds*, Topology **2** (1963), 299–340.

[14] R. Palais, *Critical point theory and the minimax principle*, Global Analysis, Proc. Symp. Pure Math. XV (1970), 185–212.

[15] S. T. Roweis and L. K. Saul, *Nonlinear dimensionality reduction by locally linear embedding*, Science **290** (2000), 2323–2326.

[16] E. Sharon, A. Brandt, and R. Basri, *Completion energies and scale*, IEEE Trans. Pattern Analysis and Machine Intelligence **22** (2000), 1117–1131.

[17] C. Truesdell, *The influence of elasticity on analysis: the classical heritage*, Bull. Amer. Math. Soc. **9** (1983), 293–310.

[18] I. Weiss, *3D Shape representation by contours*, Computer Vision, Graphics, and Image Processing **41** (1988), 80–100.

[19] L. R. Williams and D. W. Jacobs, *Stochastic completion fields: a neural model of illusory contour shape and salience*, Neural Computation **9** (1997), 837–858.

[20] Y. Wen, *Curve straightening flow deforms closed plane curves with nonzero rotation number to circles*, J. Differential Equations **120** (1995), 89–107.